# Electronic Supplementary Information for

# Stabilisation of Lanthanum Nickelate Electrocatalysts via Pt-doping for High Current Density Rechargeable Zinc-Air Battery

Wei Jian Sim,[a] Mai Thanh Nguyen,[b,*] Wathanyu Kao-ian,[c] Pinit Kidkhunthod,[c,d] Te-Wei Chiu,[e] Soorathep Khaewhom,[c] Ying-Chih Pu,[f] and Tetsu Yonezawa[b,c*]

[a]Graduate School of Engineering, Hokkaido University, Kita 13 Nishi 8, Kita-ku, Sapporo, Hokkaido 060-8628, Japan

[b]Division of Materials Science and Engineering, Faculty of Engineering, Hokkaido University, Kita 13 Nishi 8, Kita-ku, Sapporo, Hokkaido 060-8628, Japan

[c]Department of Chemical Engineering, Faculty of Engineering, Chulalongkorn University, Payathai Road Pathumwan, Bangkok 10330, Thailand

[d]Synchrotron Light Research Institute, 111 University Avenue, Muang District, Nakhon Ratchasima 30000, Thailand

[e]Department of Materials and Mineral Resources Engineering, National Taipei University of Technology, Taipei 10608, Taiwan

[f] Department of Materials Science, National Tainan University, Tainan 70005, Taiwan

*Corresponding Author, email: mai_nt@eng.hokudai.ac.jp, tetsu@eng.hokudai.ac.jp

**Table of content**

**Figure S1.** XRD patterns of $LaNiO_3$ (blue), $LaNi_{0.95}Pd_{0.05}O_3$ (orange), $LaNi_{0.95}Pt_{0.05}O_3$ (green), $LaNi_{0.80}Pt_{0.20}O_3$ (red). Patterns of rhombohedral $LaNiO_3$ (ICDD #033-0711), cubic $LaNiO_3$ (ICDD #033-0710) and platinum metal (ICDD #004-0802) included as reference.

**Figure S2.** Close-up of XRD patterns around (110) of $LaNiO_3$ (blue), $LaNi_{0.95}Pd_{0.05}O_3$ (orange), $LaNi_{0.95}Pt_{0.05}O_3$ (green), $LaNi_{0.80}Pt_{0.20}O_3$ (red). Patterns of rhombohedral $LaNiO_3$ (ICDD #033-0711) and cubic $LaNiO_3$ (ICDD #033-0710) included as reference.

**Figure S3.** Diffraction patterns and EDS spectra of the circled area on Figure 3. Top: $LaNiO_3$. Middle: $LaNi_{0.95}Pd_{0.05}O_3$. Bottom: $LaNi_{0.95}Pt_{0.05}O_3$. Cu signals are due to the use of copper TEM grid.

**Figure S4.** HAADF image of (left to right) $LaNiO_3$, $LaNi_{0.95}Pd_{0.05}O_3$, $LaNi_{0.95}Pt_{0.05}O_3$. $LaNi_{0.80}Pt_{0.20}O_3$

**Figure S5**. Extended plot of ZAB cycling test with $LaNiO_3$, $LaNi_{0.95}Pt_{0.05}O_3$ and Pt/C $IrO_2$ included as reference. ZAB cycling tests for the perovskite catalysts were stopped after 43 cycles as discharging was no longer achieving 60 mA $cm^{-2}$.

**Figure S6.** Long-term stability test by CV for $LaNiO_3$. Cycle numbers from 1 to 5000 are indicated by the colours in the legend.

**Figure S7.** Long-term stability test by CV for $LaNi_{0.95}Pt_{0.05}O_3$. Cycle numbers from 1 to 5000 are indicated by the colours in the legend.

**Figure S8.** Long-term stability test by CV for reference catalyst Pt/C + $IrO_2$. Cycle numbers from 1 to 5000 are indicated by the colours in the legend.

**Figure S9.** OER LSV of $LaNiO_3$ (blue), $LaNi_{0.95}Pt_{0.05}O_3$(red) and Pt/C + $IrO_2$(green) before and after long-term stability tests.

**1. Goldschmidt Tolerance Factor**

**Table S1.** Ionic radii and calculated Goldschmidt Tolerance Factor for each sample

**2. ORR Mechanism determination with Rotating Ring Disc Electrode (RRDE)**

**3. Fitted EXAFS parameters**

**Table S2.** Structural parameters by EXAFS fitting of $LaNiO_3$, $LaNi_{0.95}Pt_{0.05}O_3$ and $LaNi_{0.95}Pd_{0.05}O_3$ based on the Ni-O coordination number of 6 and La-O coordination number of 12.

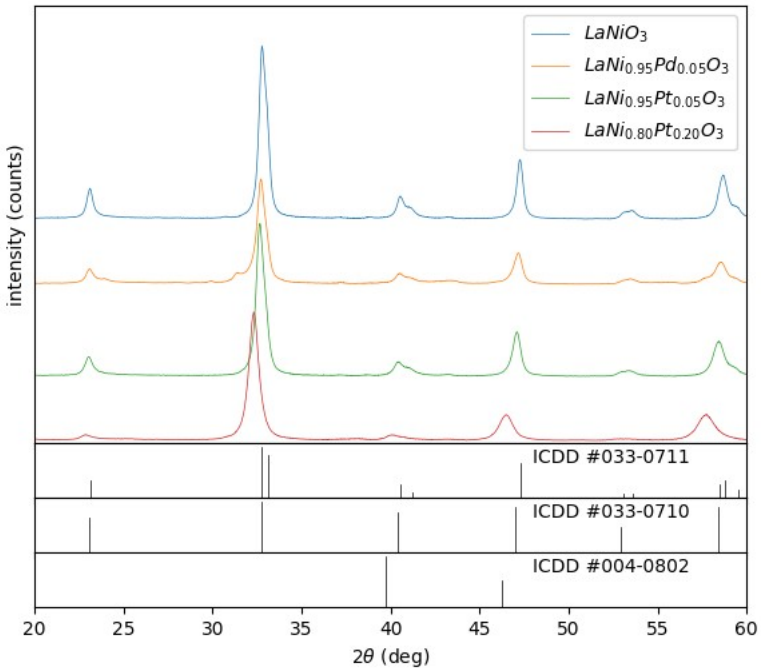


**Figure S1.** XRD patterns of $LaNiO_3$ (blue), $LaNi_{0.95}Pd_{0.05}O_3$ (orange), $LaNi_{0.95}Pt_{0.05}O_3$ (green), $LaNi_{0.80}Pt_{0.20}O_3$ (red). Patterns of rhombohedral $LaNiO_3$ (ICDD #033-0711), cubic $LaNiO_3$ (ICDD #033-0710) and platinum metal (ICDD #004-0802) included as reference.

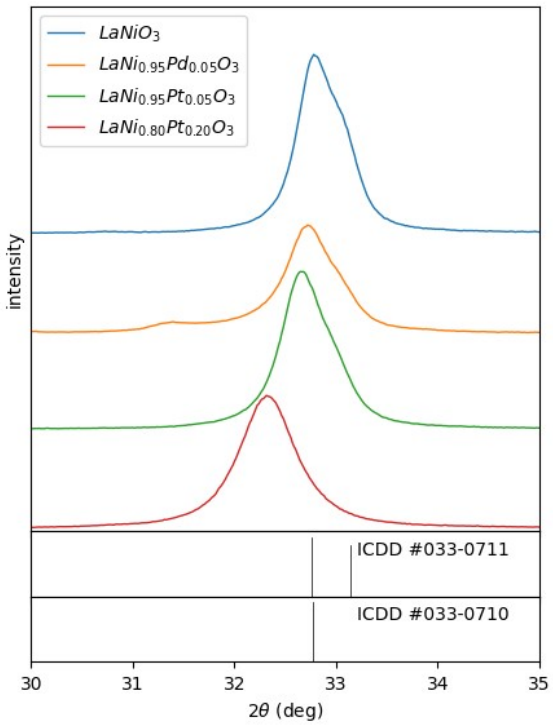


**Figure S2.** Close-up of XRD patterns around (110) of $LaNiO_3$ (blue), $LaNi_{0.95}Pd_{0.05}O_3$ (orange), $LaNi_{0.95}Pt_{0.05}O_3$ (green), $LaNi_{0.80}Pt_{0.20}O_3$ (red). Patterns of rhombohedral $LaNiO_3$ (ICDD #033-0711) and cubic $LaNiO_3$ (ICDD #033-0710) included as reference.

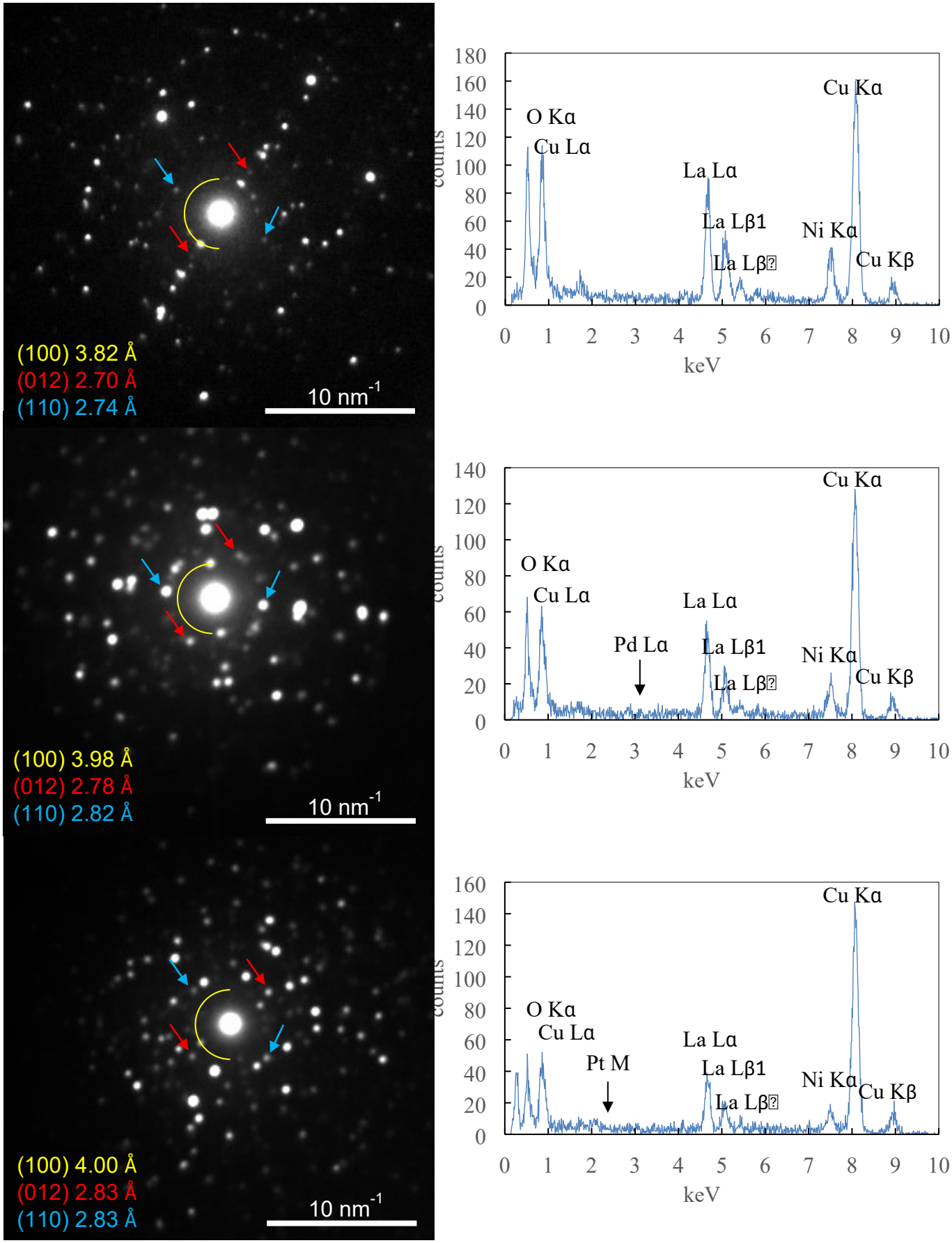


**Figure S3.** Diffraction patterns and EDS spectra of the circled area on Figure 3. Top: $LaNiO_3$. Middle: $LaNi_{0.95}Pd_{0.05}O_3$. Bottom: $LaNi_{0.95}Pt_{0.05}O_3$. Cu signals are due to the use of copper TEM grid.

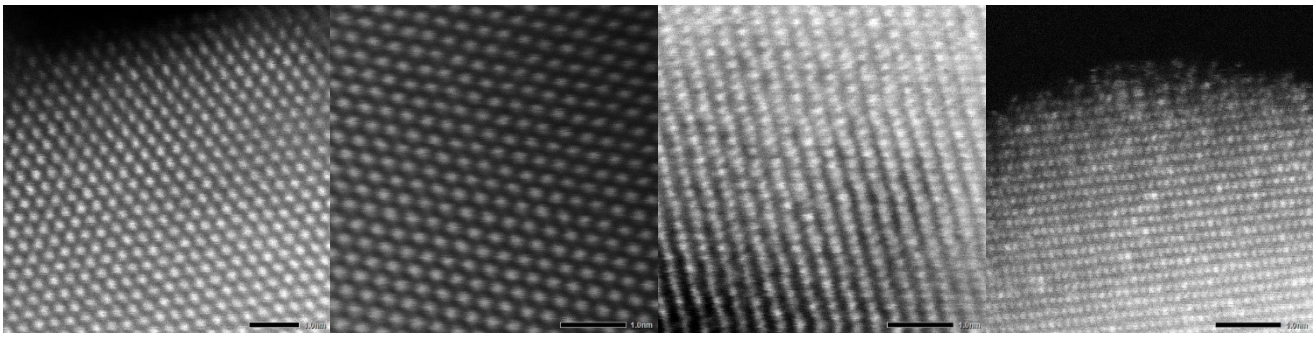

**Figure S4**. HAADF image of (left to right) $LaNiO_3$, $LaNi_{0.95}Pd_{0.05}O_3$, $LaNi_{0.95}Pt_{0.05}O_3$. $LaNi_{0.80}Pt_{0.20}O_3$. Scale bar (bottom right of each image) is 1.0 nm.

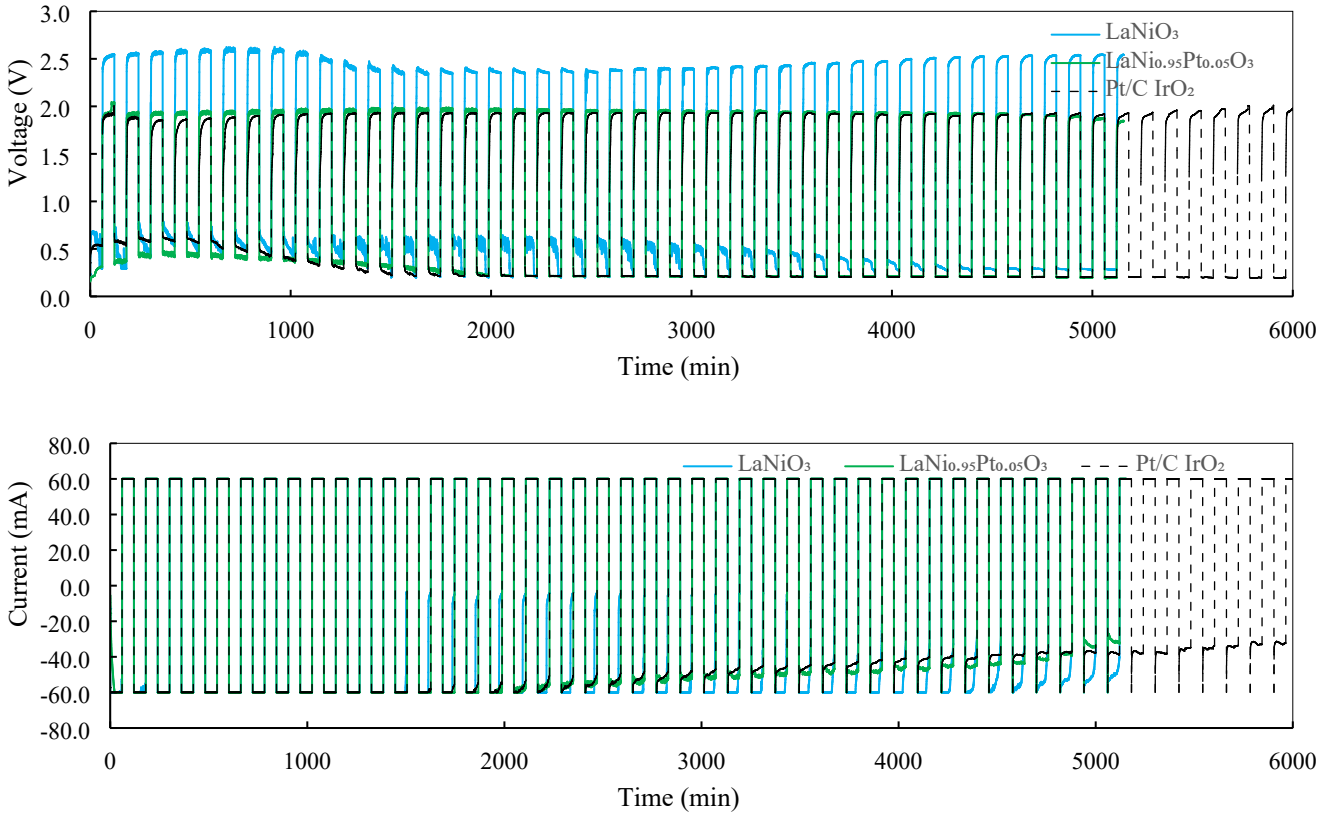


**Figure S5**. Extended plot of ZAB cycling test with $LaNiO_3$, $LaNi_{0.95}Pt_{0.05}O_3$ and Pt/C $IrO_2$ included as reference. ZAB cycling tests for the perovskite catalysts were stopped after 43 cycles as discharging was no longer achieving 60 mA $cm^{-2}$.

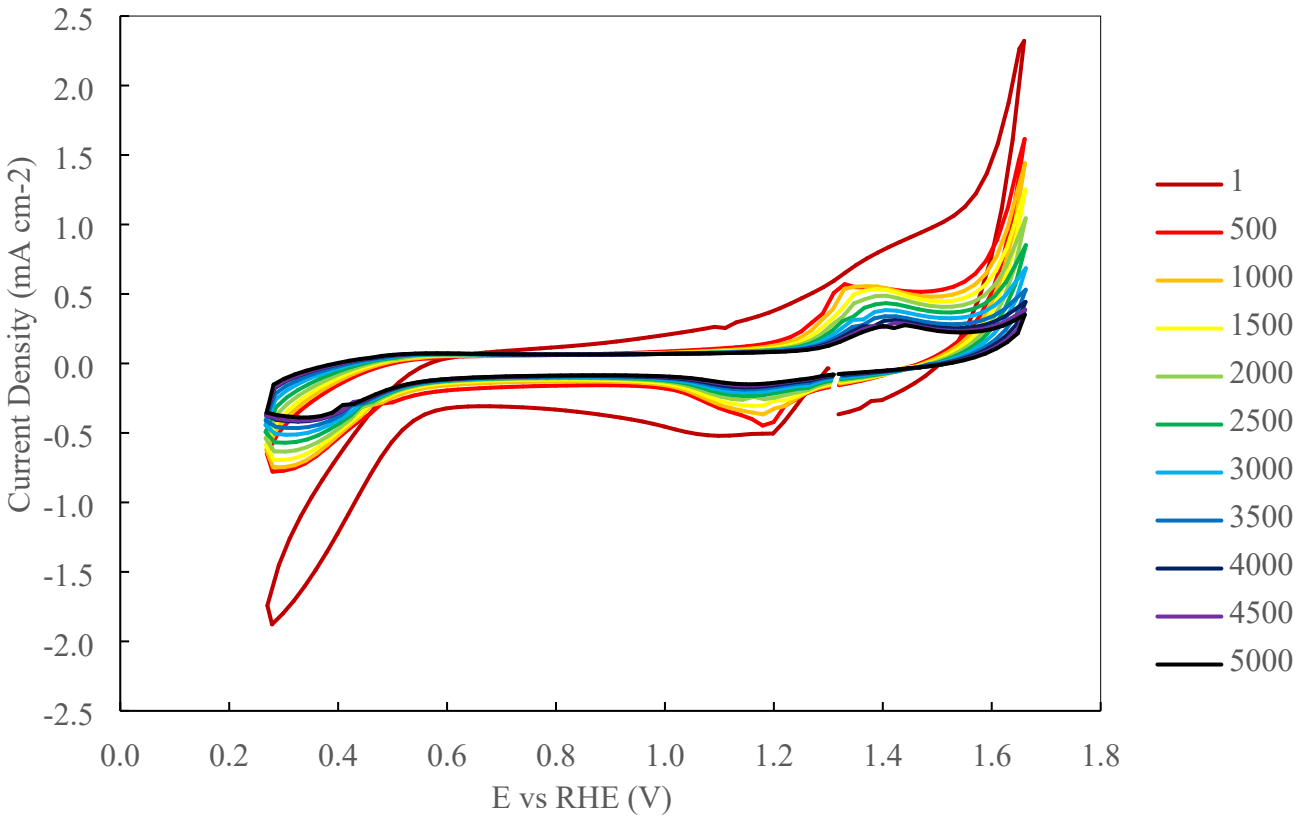


**Figure S6.** Long-term stability test by CV for $LaNiO_3$. Cycle numbers from 1 to 5000 are indicated by the colours in the legend.

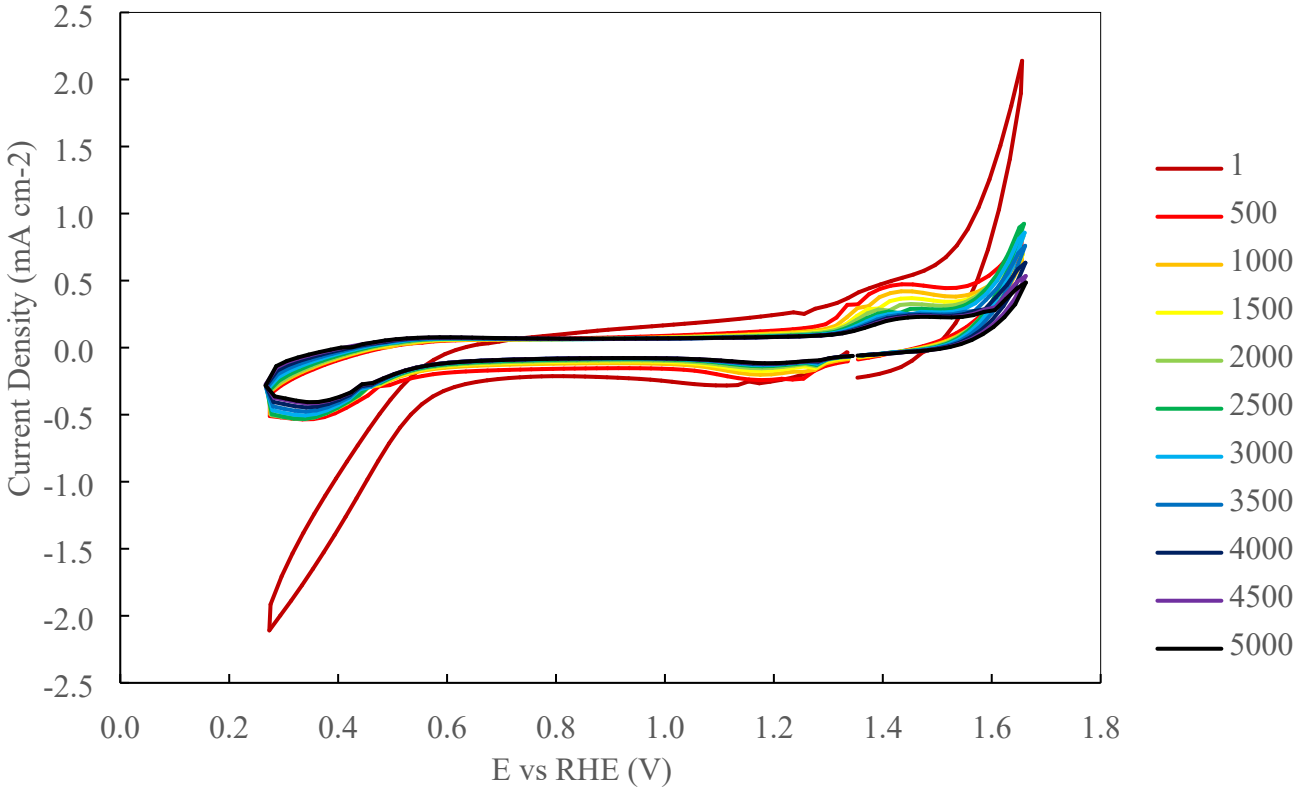


**Figure S7.** Long-term stability test by CV for $LaNi_{0.95}Pt_{0.05}O_3$. Cycle numbers from 1 to 5000 are indicated by the colours in the legend.

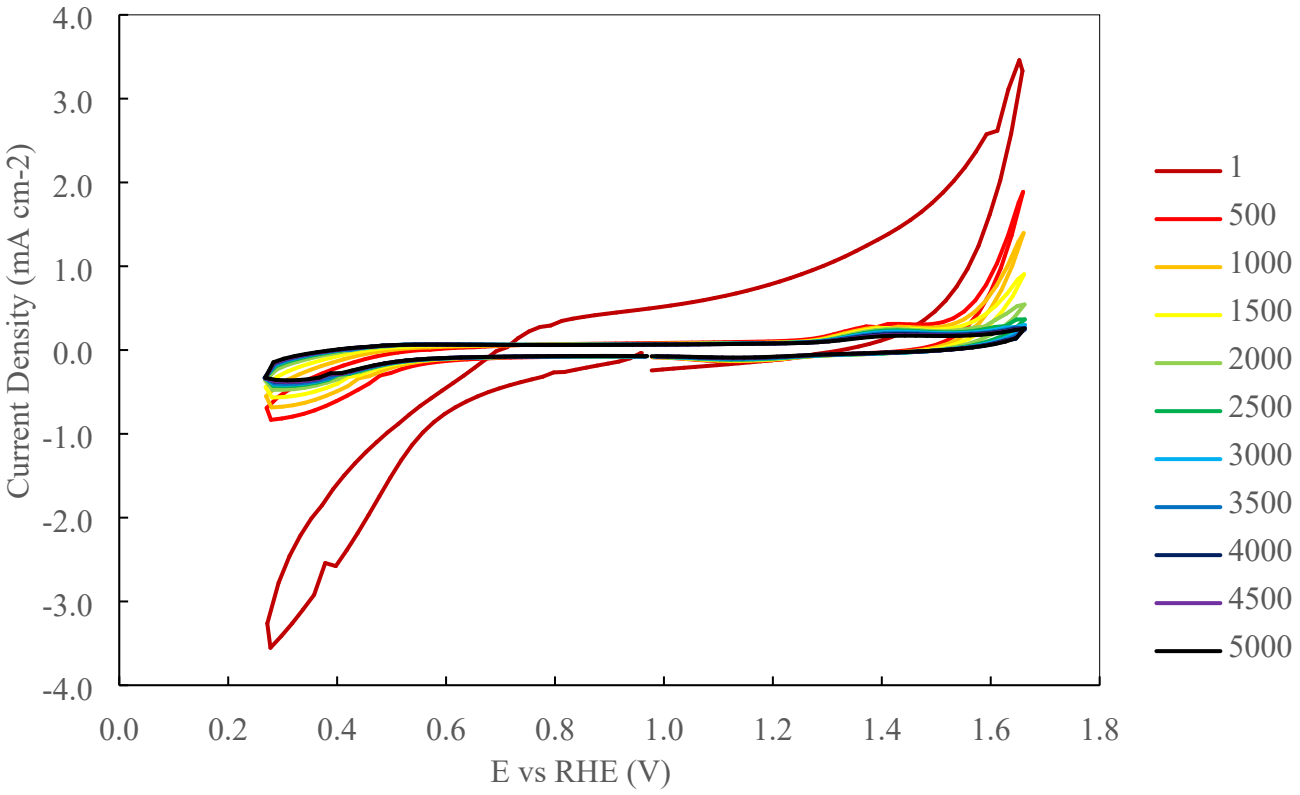


**Figure S8.** Long-term stability test by CV for reference catalyst Pt/C + $IrO_2$. Cycle numbers from 1 to 5000 are indicated by the colours in the legend.

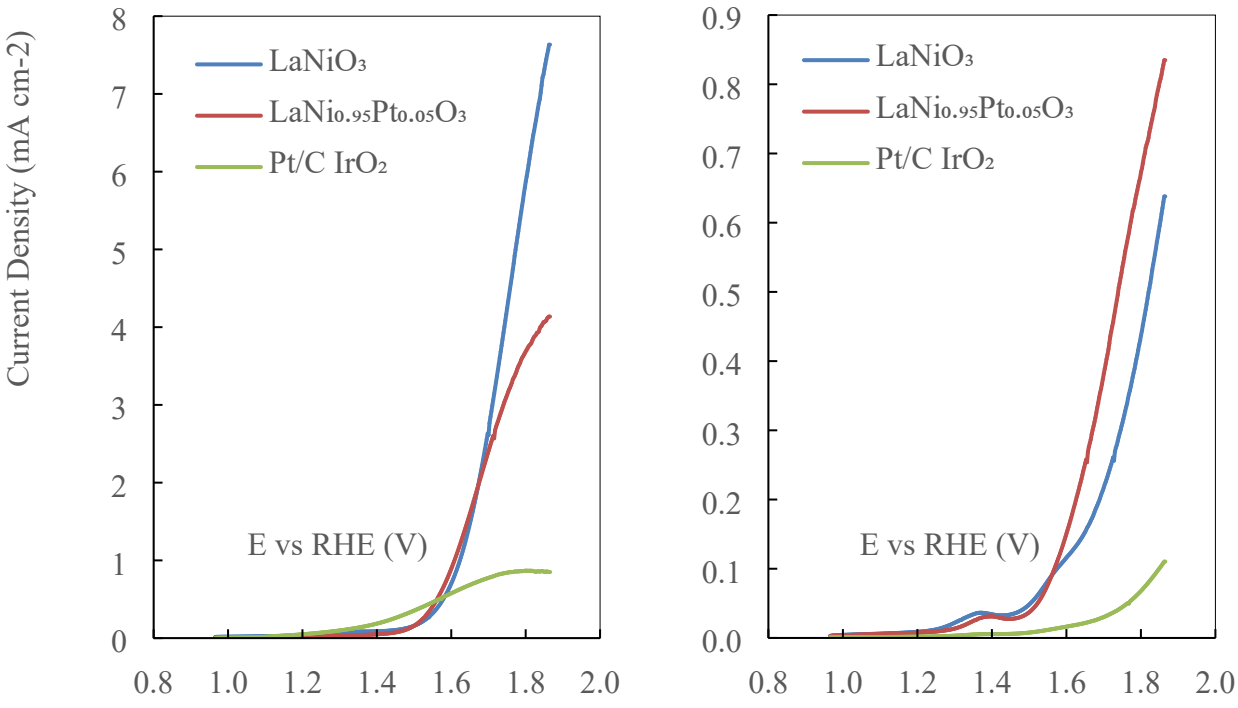


**Figure S9.** OER LSV of $LaNiO_3$ (blue), $LaNi_{0.95}Pt_{0.05}O_3$(red) and Pt/C + $IrO_2$(green) before and after long-term stability tests.

## 1. Goldschmidt Tolerance Factor

$$t = \frac{r_A + r_O}{\sqrt{2}(r_B + r_O)}$$

$r_A$ is the radius of the A cation.
$r_B$ is the radius of the B cation.
$r_O$ is the radius of the anion (usually oxygen).

**Table S1.** Ionic radii and calculated Goldschmidt Tolerance Factor for each sample

| Sample | $r_A$ | $r_{B1}$ | $r_{B2}$ | $r_{Bavg}$ | $r_O$ | t |
|---|---|---|---|---|---|---|
| $LaNiO_3$ | 1.36 | 0.56 | - | 0.56 | 1.40 | 0.9957 |
| $LaNi_{0.95}Pd_{0.05}O_3$ | 1.36 | 0.56 | 0.615 | 0.56275 | 1.40 | 0.9943 |
| $LaNi_{0.95}Pt_{0.05}O_3$ | 1.36 | 0.56 | 0.625 | 0.56325 | 1.40 | 0.9941 |
| $LaNi_{0.80}Pt_{0.20}O_3$ | 1.36 | 0.56 | 0.625 | 0.573 | 1.40 | 0.9892 |

units: Å

## 2. ORR Mechanism determination with Rotating Ring Disc Electrode (RRDE)

In a rotating ring disc electrode (RRDE) setup, the selectivity of ORR mechanism is represented by the Electron Transfer Number, n, as follows:

$$n = \frac{4I_d N}{I_d N + I_r}$$

where $I_d$ is current at the disc electrode, $I_r$ is current at the ring electrode, and N is the collection efficiency which is dependent on and specific to the geometry of the RRDE. Collection efficiency, N, has been determined in preliminary tests using potassium ferrocyanide($[Fe(CN)_6]^{4-}$)/ferricyanide($[Fe(CN)_6]^{3-}$) to be 0.48.

## 3. Fitted EXAFS parameters

**Table S2.** Structural parameters by EXAFS fitting of $LaNiO_3$, $LaNi_{0.95}Pt_{0.05}O_3$ and $LaNi_{0.95}Pd_{0.05}O_3$ based on the Ni-O coordination number of 6 and La-O coordination number of 12.

| Sample | Path | N | $S_0^2$ | $\sigma^2$ | $E_0$ | R |
|---|---|---|---|---|---|---|
| $LaNiO_3$ | Ni-O | 6.0 | 0.602 | 0.00243 | -2.516 | 1.92920 |
| $LaNi_{0.95}Pt_{0.05}O_3$ | Ni-O | 6.0 | 0.601 | 0.00159 | -2.742 | 1.93886 |
| $LaNi_{0.95}Pd_{0.05}O_3$ | Ni-O | 6.0 | 0.571 | 0.00238 | -3.888 | 1.93932 |

| Sample | Path | N | $S_0^2$ | $\sigma^2$ | $E_0$ | R |
|---|---|---|---|---|---|---|
| $LaNiO_3$ | La-O | 12.0 | 0.850 | 0.00211 | 1.353 | 2.98411 |
| $LaNi_{0.95}Pt_{0.05}O_3$ | La-O | 12.0 | 0.750 | 0.00119 | 1.725 | 2.98765 |
| $LaNi_{0.95}Pd_{0.05}O_3$ | La-O | 12.0 | 0.750 | 0.00415 | -0.287 | 2.94876 |

$S_0^2$ – Passive Electron Reduction Factor
$\sigma^2$ – Mean-Square Displacement (also known as Debye-Waller factor) representing disorder
$E_0$ – Energy Shift
R – Bond Distance